LAWRENCE
LIVERMORE
NATIONAL
LABORATORY

LLNL-TR-700477

Design and testing of microfabricated surgical tools for large animal probe insertion

S. Jorgensen

August 15, 2016

Disclaimer

This document was prepared as an account of work sponsored by an agency of the United States government. Neither the United States government nor Lawrence Livermore National Security, LLC, nor any of their employees makes any warranty, expressed or implied, or assumes any legal liability or responsibility for the accuracy, completeness, or usefulness of any information, apparatus, product, or process disclosed, or represents that its use would not infringe privately owned rights. Reference herein to any specific commercial product, process, or service by trade name, trademark, manufacturer, or otherwise does not necessarily constitute or imply its endorsement, recommendation, or favoring by the United States government or Lawrence Livermore National Security, LLC. The views and opinions of authors expressed herein do not necessarily state or reflect those of the United States government or Lawrence Livermore National Security, LLC, and shall not be used for advertising or product endorsement purposes.

This work performed under the auspices of the U.S. Department of Energy by Lawrence Livermore National Laboratory under Contract DE-AC52-07NA27344.

Design and testing of microfabricated surgical tools for large animal probe insertion

By Shelly Jorgensen

August 5, 2016

ABSTRACT

Neural probes provide therapeutic stimulation for neuropsychiatric disorders or record neural activity to investigate the workings of the brain. Researchers utilize 6 mm long temporary silicon stiffeners attached with biodissolvable adhesive to insert flexible neural probes into rat brains, but increasing the probe length fivefold makes inserting large animal probes a significant challenge because of an increased potential for buckling. This study compared the insertion success rates of 6 mm and 30 mm long silicon stiffeners that were 80 µm wide and 30 µm thick, and ascertained the material thickness and modulus of elasticity that would provide successful insertion for a 30 mm probe. Using a microdrive, stiffeners were inserted into an agarose brain phantom at controlled insertion speeds while being video-recorded. Twenty-five percent of the 30 mm silicon stiffeners fully inserted at speeds approximately four times higher than the target rate of 0.13 mm/s, while 100 percent of the 6 mm silicon stiffeners inserted successfully at target speed. Critical buckling loads (P_{cr}) were calculated for the 6 mm and 30 mm silicon stiffeners, and for 30 mm diamond and tungsten stiffeners, with thicknesses varying from 30-80 µm. . Increasing the thickness of the material by 10 µm, 20 µm and 30 µm improved the P_{cr} by 2.4, 4.7 and 8.2 times, respectively, independent of the material, and substituting diamond for silicon multiplied the buckling capacity by 5.0 times. Stiffeners made of silicon for large animal probe insertion are not strong enough to withstand buckling upon insertion without a significant increase in thickness. Replacing silicon with diamond and increasing the thickness of the stiffener to 50 µm would afford a stiffener with the same P_{cr} capacity as the 6 mm silicon stiffener that had a 100 percent insertion success rate. Experiments should continue with diamond to determine a minimum thickness that will ensure successful insertions and provide an adequate margin of safety.

INTRODUCTION

Deep brain stimulation (DBS)

Deep brain stimulation (DBS) involves implantation of neural probes with electrodes that deliver precise electrical impulses at exact locations to regulate irregular neural signals (Figure 1). DBS is used to treat several neurologic and psychiatric conditions, including Alzheimer's disease, epilepsy, major depressive disorder, obsessive-compulsive disorder and Parkinson's disease.[1,2] Researchers use DBS to record neural activity for a better understanding of brain functions, and endeavor to design probes with greater capabilities and recording lifetimes.

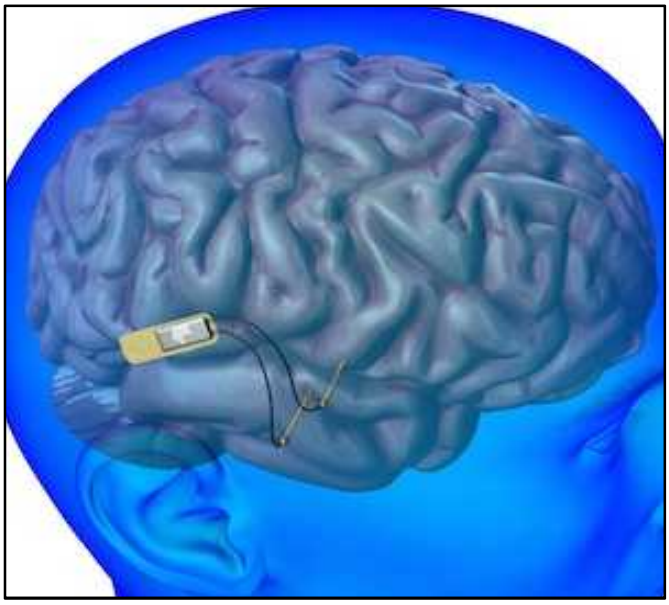

Figure 1 Diagram of brain with an implanted DBS device[3].

The insertion challenge

Researchers at Lawrence Livermore National Laboratory (LLNL) design flexible neural probes with longer *in vivo* recording times than any other neural probes currently fabricated.[4] Part of their success derives from their flexibility, because flexible probes cause less damage, as does a small cross-sectional area, but these properties make the process of inserting the probes difficult. Probes designed for rats typically require a recording depth of 6 mm, while recording depths for large animal probes are typically 30 mm. Inserting a 30 mm flexible probe presents an even greater challenge.

Innovative techniques addressing the insertion challenge abound in the literature. Eckhorn et al. designed an elastic tube to support the neural probe as it was inserted into the brain,[5] and numerous papers describe a biodissolvable delivery vehicle created by coating the probe with a substance that dissolves after implantation.[6,7,8,9,10,11] Many techniques use a temporary delivery shuttle. Loffler et al. created a probe with a reinforced punch hole for attachment to a temporary insertion rod.[12] Another technique, developed at LLNL, uses a temporary silicon stiffener attached to the neural probe with a bio-dissolvable adhesive,[13] both of which are shown in Figure 2. Po-Cheng et al. used a detachable ultrasonic enabled

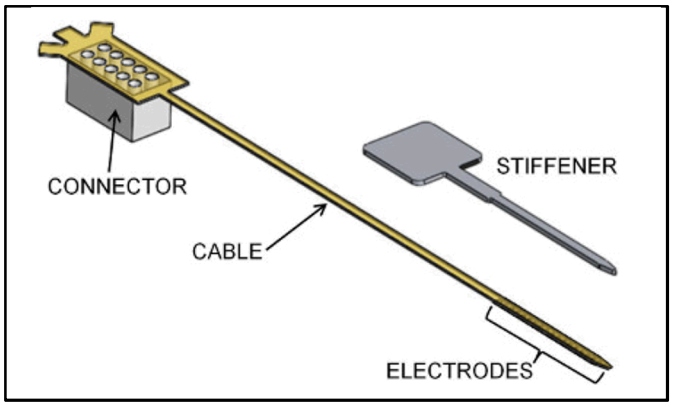

Figure 2 Drawing of neural probe and the stiffener used for insertion using technique developed by Felix et al.[13]

inserter[14] and Jaroch et al. used a magnetic insertion tip.[15] Damage to neural tissue is minimized by having a smooth surface, a small cross-sectional area, a sharp tip, and inserting the probe at a slow rate.[16,17,18,19,20] Effective techniques exist, but researchers are still working on their optimization, particularly to address the issues encountered when inserting high aspect ratio neural probes.

Insertion of an LLNL flexible neural probe, using the technique developed by Felix et al.,[13] requires the use of a temporary delivery shuttle to provide stiffness to the neural probe. There is an increased risk of buckling failure for the stiffener due to the high aspect ratio: stiffeners used for rats are typically 6 mm in length, 80 µm wide and 30 µm thick, while large animal stiffeners may be 30 mm in length, 80 µm wide and 30 µm thick. A stiffer material decreases the potential for buckling, as does increasing the cross-sectional area, but there are biocompatibility constraints on material selection and safety limitations on cross-sectional area. Biocompatible materials available for use as a delivery shuttle include silicon, tungsten and diamond with moduli of elasticity of 169 GPa,[21] 405 GPa[22] and 850 GPa,[23] respectively.

This research compared insertion success for 6 mm long silicon stiffeners (for rats) and 30 mm long stiffeners (for monkeys) using the technique created by Felix et al. (2013), and investigated the material and cross-sectional area needed to ensure a 100 percent successful insertion rate for LLNL flexible neural probes.

MATERIALS & METHODS

Materials & equipment

The stiffeners used for the experiment were fabricated from a silicon-on-insulator wafer, using standard microfabrication techniques, and had the following dimensions for length, width and thickness, respectively, 6 mm, 80 µm, 30 µm, and 30 mm, 80 µm, 30 µm. A 10 µm x 10 µm channel runs down the center to provide space for the bio-dissolvable adhesive that affixes the stiffener to the probe. Figure 3 shows an image with both stiffeners side-by-side for contrast.

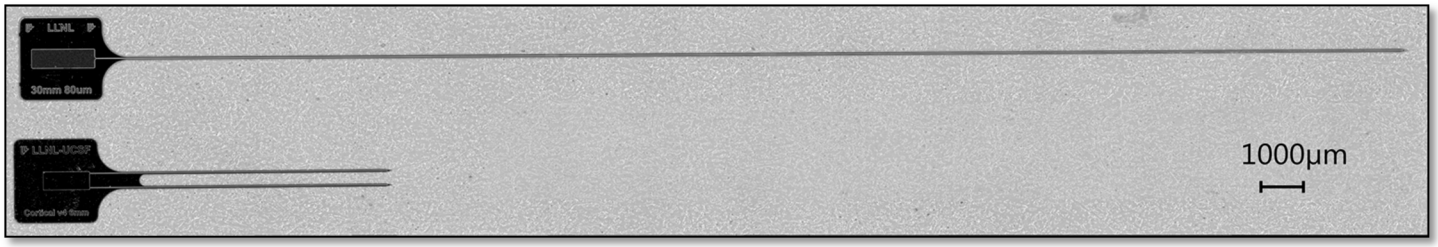

Figure 3 2D dimensional stitch of 6 mm long and 30 mm long stiffeners used in experiment (made with Keyence VHX 5000 microscope).

An acrylic box filled with 0.6% agarose gel, prepared following a standard recipe, simulated brain tissue. According to the literature, this concentration most accurately replicates brain tissue.[24] Brain phantoms were kept in a refrigerator for preservation and were stored for a maximum of 7 days.

As shown in Figure 4, stiffeners were fastened with putty (3M) onto an acrylic mounting plate assembled to fit a microdrive (CONEX-CC) that was attached to a stereotaxic frame. The microdrive software allowed selection of specific insertion speeds and distances. A microscope (Keyence VHX 5000) and a digital camera recorded images of the stiffeners as they inserted into the agarose, and the temperature of the gel was monitored using an infrared thermometer.

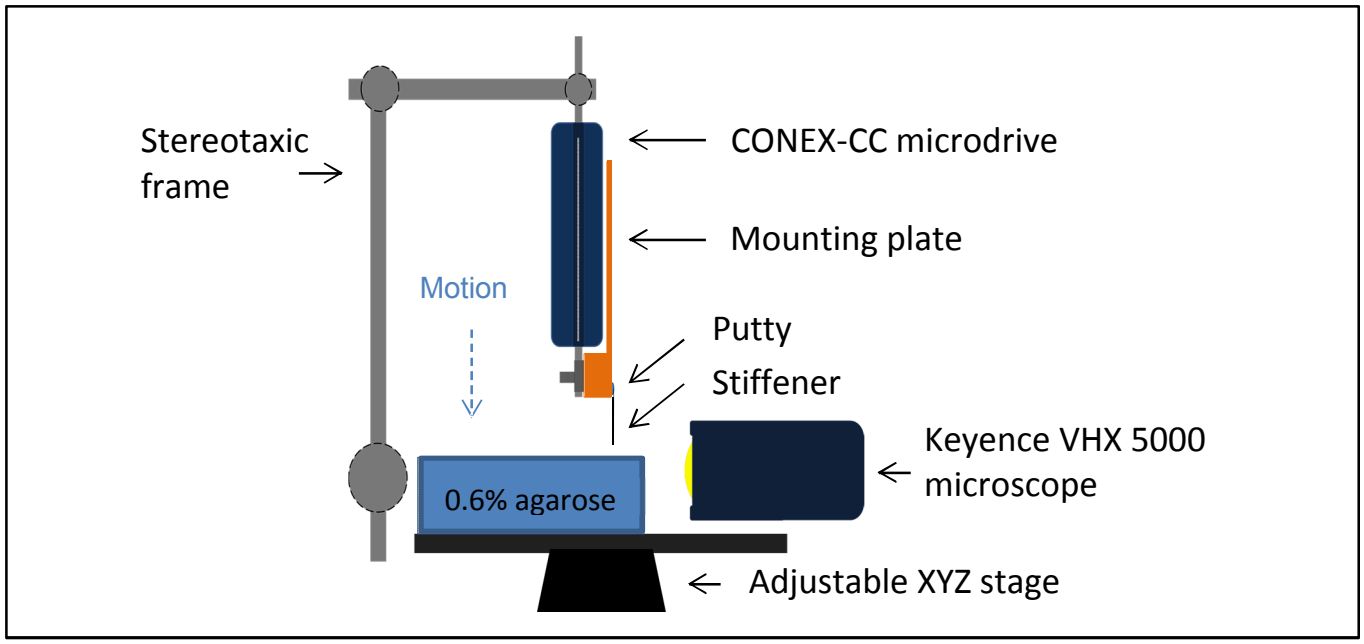

Figure 4 Diagram of experimental set up.

Experimental procedure

A 0.6% agarose gel was prepared before the experimental procedure, following the Sigma-Aldrich protocol (with hotplate), and poured into an acrylic box to cure overnight.[25] On the day of the experiment, a thin layer of phosphate buffered saline (PBS) kept the agarose hydrated while it was warmed in an oven to 37° C (body temperature). Each of the stiffeners used for the experiment was examined for tip breakage and placed in individual, labeled boxes. For the test, the tab portion of the stiffener was attached to the mounting plate with putty, and the stiffener was positioned just above the 37°C gel and about 2 mm from the edge of the acrylic box. A camera and the microscope video-recorded each experiment. The microdrive was set to insert a distance equal to the length of the stiffener at a specific speed (between 0.13 and 0.5 mm/s), and the descent was closely monitored. If the radius of curvature exceeded 10 mm, the descent of the microdrive was interrupted.

Calculations

Critical buckling load (P_{cr}) was calculated using Euler's buckling equation (Equation 1). Once the stiffener embeds in the gel it is fixed on both ends and the effective length is half of the total length, as shown on the graph in Figure 5. Effective length is measured between the inflection points of the curve. Figure 6 shows the cross-sectional area used for calculating the area moment of inertia which is calculated using Equation 2.

$$(1) \qquad P_{cr} = \pi^2 \frac{EI_x}{L_e^2}$$

Where:

P_{cr} = Critical buckling load (N)
E = Modulus of elasticity (Pa)
I_x = Area moment of inertia (m^4)
L_e = Effective length (m)

$$(2) \qquad I_x = \frac{wt^3}{12}$$

Where:

I_x = Area moment of inertia (m^4)
w = Width (m)
t = thickness (m)

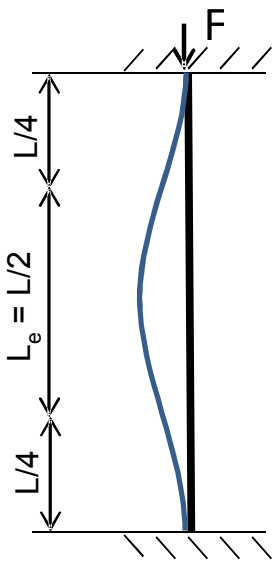

Figure 5 Diagram of buckling curve for a column fixed on both ends.

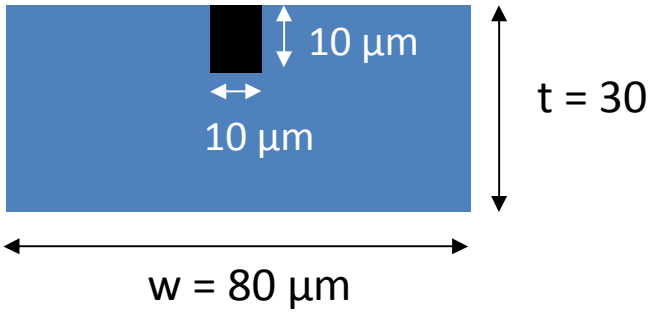

Figure 6 Cross-sectional view of stiffener showing the open channel that runs down the center of the stiffener for the biodissolvable adhesive.

RESULTS

Insertion success rate

Table 1 presents the insertion success rate for each of the silicon stiffeners tested, and Figures 7 and 8 show the deflections experienced by two different 30 mm silicon stiffeners. For the 30 mm long stiffeners, it was noted that even those that fully inserted underwent a slight deflection, but then straightened out and inserted fully (Figure 7).

Table 1 Summary of results for insertion success rate of stiffeners tested.

Material	Length (mm)	Width (µm)	Thickness (µm)	Insertion speed (mm/s)	Success rate (%)
Silicon	6	80	30	0.1-1.0	100
Silicon	30	80	30	0.4-0.5	25

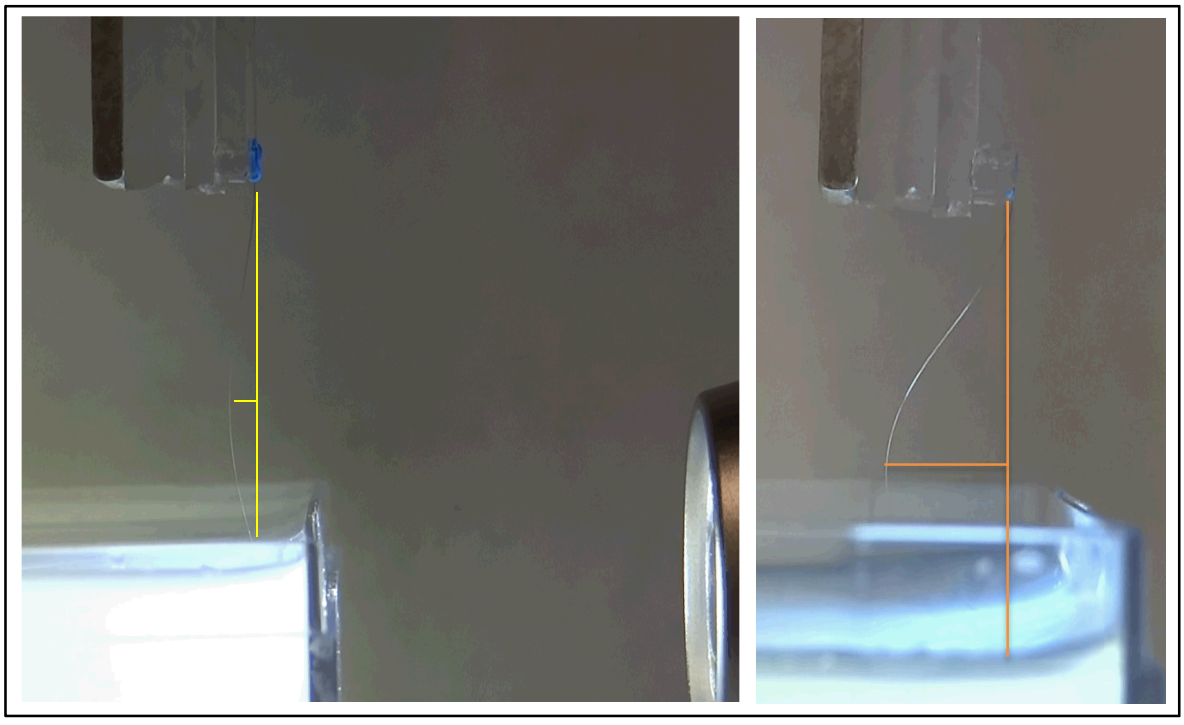

Figure 7 Image of a 30 mm silicon stiffener that inserted fully The stiffener experienced some deflection but recovered and inserted the full 30 mm.

Figure 8 Image of a 30 mm silicon stiffener that did not insert successfully.

Critical buckling load (P_{cr})

Calculations for critical buckling load (P_{cr}) for the two silicon stiffeners, with varying thickness, are graphed in Figure 9, along with the P_{cr} for 30 mm stiffeners made of tungsten and diamond. The dashed purple line marks the P_{cr} of the 6 mm stiffener that was successful 100 percent of the time.

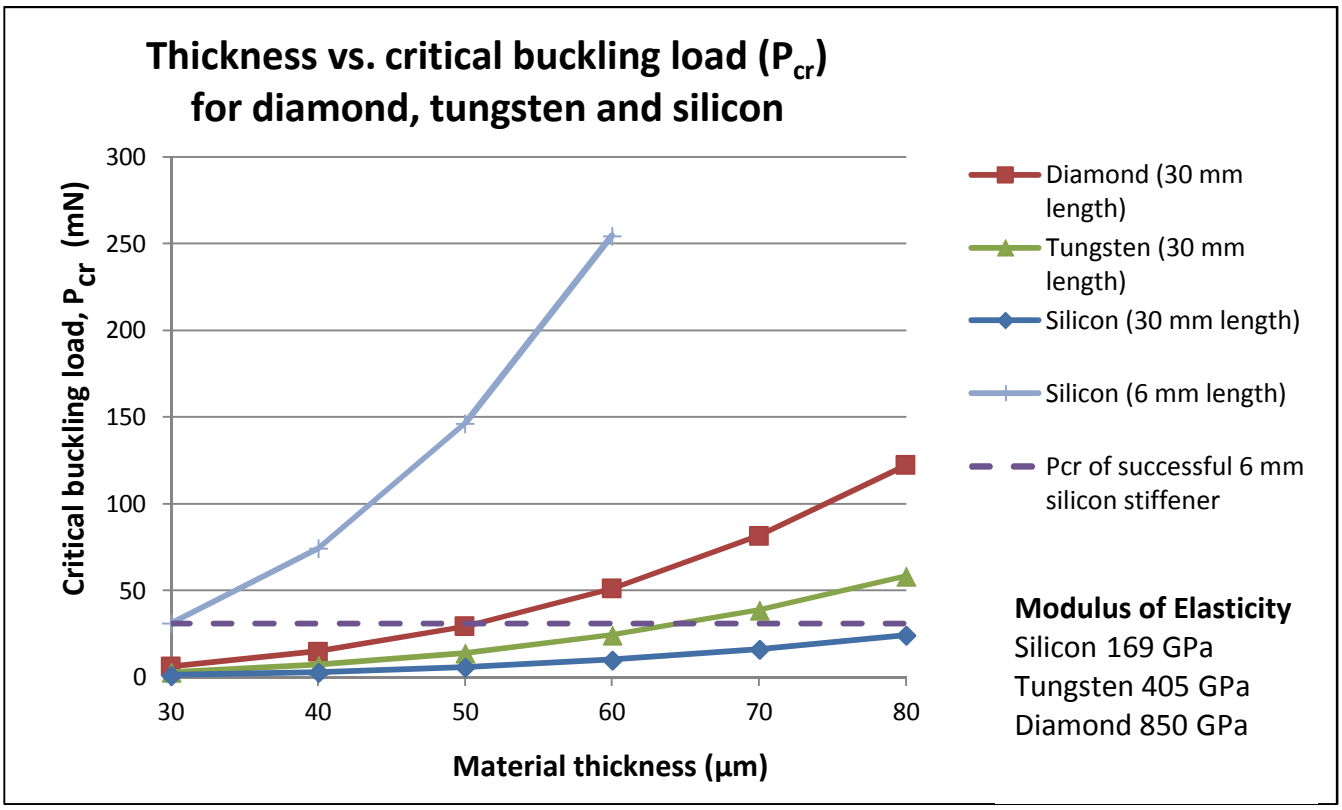

Figure 9 Graph showing the effect of thickness and material modulus of elasticity on critical buckling load

DISCUSSION

The goal for this experiment was to compare the insertion success rate of 6 mm and 30 mm silicon stiffeners and identify the requirements for a stiffener that would successfully insert a 30 mm neural probe. Insertion of a 30 mm silicon stiffener at target speed was not successful, but much was learned about how to design a 30 mm stiffener that will ensure a 100 percent successful insertion rate.

Inserting at a slow rate is desirable to decrease tissue damage, though inserting at a greater speed facilitates insertion because rate dependent material properties increase stiffness at higher speeds. The target speed for this experiment was 0.13 mm/s. Even at a speed almost ten times the target speed, there was not a consistent method that worked for inserting the 30 mm stiffeners successfully. The 6 mm stiffeners had no problems with buckling at any speed tested (0.1-1.0 mm/s) and were able to withstand multiple insertions, while the 30 mm stiffeners buckled more due to repeated insertions.

Critical buckling loads were calculated for different thicknesses of 6 mm and 30 mm long silicon stiffeners, and for comparison of 30 mm long tungsten and diamond stiffeners, all having the same width. Length is a major contributor to the critical buckling capacity of the stiffeners. P_{cr} for a 6 mm silicon stiffener is 25 times greater than the P_{cr} for a 30 mm silicon stiffener. The limiting variables for buckling in this experiment are the area moment of inertia (I_x) and the modulus of elasticity (E). Minimizing tissue damage warrants keeping the cross-sectional area as slender as possible, but has adverse effects on the P_{cr}. Increasing the thickness of the 30 mm stiffener by 10 µm, 20 µm or 30 µm increases the P_{cr} by 2.39, 4.69 and 8.2 times, respectively, for all three materials, and using diamond instead of silicon increases the P_{cr} by 5 times.

It is critical to have a high percent success rate for *in vivo* neural probe insertions. The 6 mm silicon stiffeners tested had a 100 percent success rate because they were very robust and possibly over-designed. On the graph in Figure 9 the dashed horizontal line represents the P_{cr} of the 6 mm stiffeners from the experiment. Under the assumption that having an equivalent buckling capacity would mean a similar success rate, diamond at a thickness of 50 µm would ensure a 100 percent success rate for *in vivo* probe insertions with 30 mm stiffeners. Because no buckling of the 6 mm probe was observed under relevant test conditions, it is possible that a 30 mm diamond stiffener with a reduced thickness would still provide a reliable insertion success rate.

CONCLUSION

Silicon stiffeners that are 30 mm long, 80 µm wide and 30 µm thick buckle when inserted into 0.6% agarose at the target insertion speed of 0.13 mm/s and fail to insert completely. Using a 30 mm long diamond stiffener 80 µm wide and 50 µm thick would provide a critical buckling load (P_{cr}) similar to the P_{cr} for the 6 mm silicon stiffener that had a 100 percent insertion success rate. Further experimentation should explore the minimum thickness of diamond required for a 100 percent insertion success rate while still providing a margin of safety.

ACKNOWLEDGEMENTS

I would like to thank Vanessa Tolosa and Supin Chen for their guidance in this research, and Jeanie Pebbles for her assistance and support.

Funding provided through the Department of Energy Science Undergraduate Laboratory Internship (SULI) Program was greatly appreciated.

BIBIOLGRAPHY

1. Lozano, A. M., & Lipsman, N. (2013). Probing and Regulating Dysfunctional Circuits Using Deep Brain Stimulation. *Neuron, 77*(3), 406-424. doi:10.1016/j.neuron.2013.01.020
2. Lawrence Livermore National Laboratory. *Deep Brain Stimulation to Treat Neuropsychiatric Disorders*. RetrWeb 31 July 2016. https//nuerotech.llnl.gov/projects/subnets
3. Schechter, Erik. (2014, July 14). Wireless Implant Zaps Neurons to Fight Memory Loss. Popular Mechanics. Hearst Communications. RetrWeb 31 July 2016. http://www.popularmechanics.com/science/health/a10886/a-wireless-implant-to-fight-memory-loss-16984118/
4. Chen, S. (2016, August 01). SULI report questions [E-mail interview**].**
5. Eckhorn, R., & Thomas, U. (1993). A NEW METHOD FOR THE INSERTION OF MULTIPLE MICROPROBES INTO NEURAL AND MUSCULAR TISSUE, INCLUDING FIBER ELECTRODES, FINE WIRES, NEEDLES AND MICROSENSORS. *Journal of Neuroscience Methods, 49*(3), 175-179. doi:10.1016/0165-0270(93)90121-7
6. Barz, F., Ruther, P., Takeuchi, S., Paul, O., & IEEEE. (2015). Flexible silicon-polymer neural probe rigidified by dissolvable insertion vehicle for high-resolution neural recording with improved duration. *2015 28th IEEE International Conference on Micro Electro Mechanical Systems* (pp. 636-639).
7. Gilgunn, P. J., Khilwani, R., Kozai, T. D. Y., Weber, D. J., Cui, X. T., Erdos, G. IEEE (2012). An ultra-compliant, scalable neural probe with molded biodissolvable delivery vehicle. *2012 IEEE 25th International Conference on Micro Electro Mechanical Systems*.
8. Kozai, T. D. Y., & Kipke, D. R. (2009). Insertion shuttle with carboxyl terminated self-assembled monolayer coatings for implanting flexible polymer neural probes in the brain. *Journal of Neuroscience Methods, 184*(2), 199-205. doi:10.1016/j.jneumeth.2009.08.002
9. Lecomte, A., Castagnola, V., Descamps, E., Dahan, L., Blatche, M. C., Dinis, T. M., Bergaud, C. (2015). Silk and PEG as means to stiffen a parylene probe for insertion in the brain: toward a double time-scale tool for local drug delivery. *Journal of Micromechanics and Microengineering, 25*(12). doi:10.1088/0960-1317/25/12/125003
10. Lewitus, D., Smith, K. L., Shain, W., & Kohn, J. (2011). Ultrafast resorbing polymers for use as carriers for cortical neural probes. *Acta Biomaterialia, 7*(6), 2483-2491. doi:10.1016/j.actbio.2011.02.027
11. Lo, M., Wang, S., Singh, S., Damodaran, V. B., Kaplan, H. M., Kohn, J., Zahn, J. D. (2015). Coating flexible probes with an ultra-fast degrading polymer to aid in tissue insertion. *Biomedical Micro devices, 17*(2). doi:10.1007/s10544-015-9927-z
12. Loeffler, S., Xie, Y., Detemple, P., Moser, A., & Hofmann, U. G. (2012). An implantation technique for polyimide based flexible array probes facilitating neuronavigation and chronic implantation. *Biomedical Engineering-Biomedizinische Technik, 57*(Suppl. 1).

doi:10.1515/bmt-2012-4437
13. Felix, S. H., Shah, K. G., Tolosa, V. M., Sheth, H. J., Tooker, A. C., Delima, T. L., Pannu, S. S. (2013). Insertion of flexible neural probes using rigid stiffeners attached with a biodissolvable adhesive. Jove-Journal of Visualized Experiments (79). doi:10.3791/50609
14. Po-Cheng, C., & Lal, A. (2015). *Detachable ultrasonic enabled inserter for neural probe insertion using biodissolvable polyethylene glycol*. 18th International Conference on Solid-State Sensors, Actuators and Microsystems
15. Jaroch, D. B., Irazoqui, P., & Rickus, J. L. (2014). US 08761898.
16. Kamaraj, A. B., Sundaram, M. M., & Mathew, R. (2013). Ultra-high aspect ratio penetrating metal microelectrodes for biomedical applications. *Microsystem Technologies-Micro-and Nanosystems-Information Storage and Processing Systems, 19*(2), 179-186. doi:10.1007/s00542-012-1653-3
17. Fekete, Z., Nemeth, A., Marton, G., Ulbert, I., & Pongracz, A. (2015). Experimental study on the mechanical interaction between silicon neural microprobes and rat dura mater during insertion. *Journal of Materials Science-Materials in Medicine, 26*(2). doi:10.1007/s10856-015-5401-y
18. Lee, S., Kanno, S., Kino, H., & Tanaka, T. (2013). Study of Insertion Characteristics of Si Neural Probe with Sharpened Tip for Minimally Invasive Insertion to Brain. *Japanese Journal of Applied Physics, 52*(4). doi:10.7567/jjap.52.04cl04
19. Sanghoon, L., Kanno, S., Kino, H., & Tanaka, T. (2013). Study of insertion characteristics of Si neural probe with sharpened tip for minimally invasive insertion to brain. *Japanese Journal of Applied Physics, 52*(4), 04CL04 (05 pp.)-04CL04 (05 pp.). doi:10.7567/jjap.52.04c104
20. Welkenhuysen, M., Andrei, A., Ameye, L., Eberle, W., & Nuttin, B. (2011). Effect of Insertion Speed on Tissue Response and Insertion Mechanics of a Chronically Implanted Silicon-Based Neural Probe. *IEEE Transactions on Biomedical Engineering, 58*(11), 3250-3259. doi:10.1109/tbme.2011.2166963
21. Hopcroft, M. A., Nix, W. D., Kenny, T. W. (2010). What is the Young's modulus of silicon? *Journal of microelectromechanical systems 19(2), 229-238*.
22. Hertzberg, R. W. (2012). Deformation and Fracture Mechanics of Engineering Materials, 5th Edition. Wiley (Table 7.1). RetrWeb 03 August 2016. http://www.wiley.com/WileyCDA/WileyTitle/productCd-EHEP002042.html>
23. Advanced Diamond Technologies Inc. (2010). *UNCD Wafers* Data Sheet and Technical Knowledge Bank. (p. 14).
24. Chen, Z. et al. (2004). A realistic brain tissue phantom for intraparenchymal infusion studies. *Journal of Neurosurgery.* 101 **(**2), 314-322.
25. Agarose Product Information. (1996, October 26). Retrieved June 28, 2016, from http://www.sigmaaldrich.com/content/dam/sigma-aldrich/docs/Sigma/Product_Information_Sheet/a9539pis.pdf

This work performed under the auspices of the U.S. Department of Energy by Lawrence Livermore National Laboratory under Contract DE-AC52-07NA27344.